Uric Acid Dihydrate Revisited

SEAN PARKIN[a]*† AND HÅKON HOPE[b]

[a]*Molecular and Structural Biology Division, Biology and Biotechnology Research Program, Lawrence Livermore National Laboratory, Livermore, CA 94550, USA, and* [b]*Department of Chemistry, University of California at Davis, Davis, CA 95616, USA. E-mail: sean@xray.duke.edu*
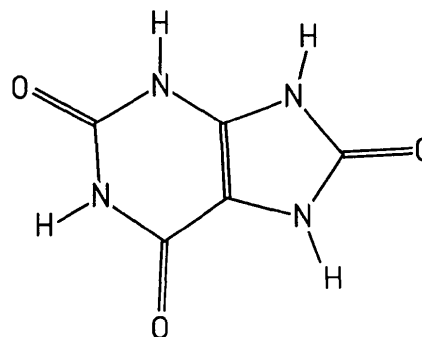
Abstract

At 120 K, crystals of pure laboratory-grown uric acid dihydrate [7,9-dihydro-1H-purine-2,6,8(3H)-trione dihydrate], $C_5H_4N_4O_3.2H_2O$, are monoclinic, $P2_1/c$, with a = 7.237 (3), b = 6.363 (4), c = 17.449 (11) Å, β = 90.51 (1)°, Z = 4, wR_2 (all data) = 0.1094, R_1 = 0.0406 for data with $I > 2\sigma(I)$. The crystals exhibit pseudo-orthorhombic twinning with refined twin fractions of 0.89 and 0.11. Within each twin, disorder about a noncrystallographic twofold exists with refined occupancies of 0.83 and 0.17. Packing consists of layers of hydrogen-bonded uric acid separated by layers of hydrogen-bonded water. The epitaxy of uric acid dihydrate with its anhydrous counterpart is readily explicable from the refined model. Treatment of the structure as twinned and disordered in space group $P2_1/c$ fully accounts for well documented violations of systematic absences in orthorhombic space groups.

1. Introduction

Uric acid [7,9-dihydro-1H-purine-2,6,8(3H)-trione dihydrate, UA], a major constituent of some mammalian calculi, crystallizes in two known forms, a stable anhydrous monoclinic form (AUA) and a poorly characterized form consistently described as orthorhombic (Ringertz, 1965, 1966; Lonsdale & Mason, 1966; Shirley, 1966; Sutor & Scheidt, 1968; Rinaudo & Boistelle, 1980). The crystal structure of AUA was published over 30 years ago by Ringertz (1966), but further single crystal work on the dihydrate (UAD) has only recently appeared (Artioli *et al.*, 1997, hereafter AMG). AMG described refinement of the structure of crystals from human bladder stones in the orthorhombic space group *Pnab* (a nonstandard setting of *Pbcn*). Their model forces a 50:50 disordering of UA, which superimposes the six- and five-membered rings. The resulting average structure is severely distorted, with a number of grossly deviant bond lengths and angles. Inconsistent systematic absences that precluded space-group assignment in previous work (Ringertz, 1965) were also

---

† Present address: Biochemistry Department, Duke University, Durham, NC 27710, USA.

apparent, but were attributed to short-range ordering by AMG on the scale of a few unit cells.

Notwithstanding the similar cell dimensions, there are real differences between laboratory-grown UAD crystals and those from human urinary deposits. A striking observation is that laboratory grown crystals are very unstable, tending to rapidly lose water and transform to the anhydrous modification, while pathological specimens can be very stable. Synthetic crystals are colorless, while those from human stones cover a range of yellows and oranges (AMG). There are also differences in the relative strengths of various classes of reflection, specifically the systematic absence violators of *Pnab* (after transformation to our cell setting). Refinement of the transformed AMG model against our data after forced merging into the Laue group *mmm* (R_{int} = 0.251) was not satisfactory.

2. Experimental details

2.1. Crystal growth and mounting

Reagent-grade UA (Aldrich Chemical Co., St Louis, MO) was dissolved in boiling distilled water (20 mg per 100 ml, acidified to pH 3.5 with acetic acid). Portions of this solution were rapidly cooled and observed under a microscope. A thin-wedge-shaped crystal (~0.30 × 0.30 × 0.01 mm) was transferred to oil (Paratone N, Exxon Corporation), as described by Hope (1987), and the aqueous layer was gently removed. The crystal suffered numerous cracks and breaks during attempts to mount it and the thin edge was visibly bent. An

irregular fragment roughly three-quarters its initial size was mounted and transferred to the cold-stream path of a modified Siemens LT-2 attached to a Siemens P4RA diffractometer.

2.2. Systematic absences, indexing and space-group assignment

Initial indexing at 120 K gave approximately orthorhombic metrics, but a search for strong reflections between $45 < 2\theta < 55°$ to refine the cell revealed systematic absences inconsistent with any orthorhombic space group. Intensity statistics for reflections that correspond to the n and a glide planes in the AMG structure were somewhat weaker than average, but not dramatically so. Mean $I/\sigma(I)$ for 'n' and 'a' violators (of the AMG setting) were 14.1 and 5.6, compared with 16.8 overall. The 'b' glide of AMG corresponds to the c glide in our setting and was very clear from the intensity statistics [mean $I/\sigma(I) = 0.9$]. The cell was refined against 24 reflections well distributed in reciprocal space, revealing two angles at 90° within the standard uncertainties (s.u.) and one of 90.51 (1)°. The true crystal system was thus identified as monoclinic with $a = 7.237$ (3), $b = 6.363$ (4), $c = 17.449$ (11) Å, $\beta = 90.51$ (1)° and the space group was unambiguously assigned as $P2_1/c$, with no significant systematic absence violations. There are differences between our cell dimensions and those (after transformation) in AMG [$a = 7.409$ (1), $b = 6.332$ (1), $c = 17.559$ (3) Å]. The cell volume contraction of ~2.5% is typical for molecular crystals on cooling, but was not isotropic. The observed deviation of β from 90° may also have been enhanced by the transition to low temperature.

2.3. Data collection

Reflections were split due to twinning and cracking, especially at high diffraction angle. The ω-scan technique was used for data collection despite the Ni-filtered Cu $K\alpha$ radiation so as to prevent truncation errors due to reflection width. The possibility of incorrect treatment of backgrounds resulting from ω scans was investigated and found to be minor. An initial data collection at a scan rate of 60° min^{-1} produced a very weak dataset so a second, much stronger set was collected from the same crystal. Data collection and processing statistics for set 2 are given in Table 1.†

3. Structure solution and refinement

The structure was solved by direct methods (TREF in SHELXTL; Sheldrick, 1984) using dataset 1, but

† Lists of atomic coordinates, anisotropic displacement parameters and structure factors have been deposited with the IUCr (Reference: BK0050). Copies may be obtained through The Managing Editor, International Union of Crystallography, 5 Abbey Square, Chester CH1 2HU, England.

Table 1. *Experimental details*

Crystal data

Chemical formula	$C_5H_4N_4O_3.2H_2O$
Chemical formula weight	204.15
Cell setting	Monoclinic
Space group	$P2_1/c$
a (Å)	7.237 (3)
b (Å)	6.363 (4)
c (Å)	17.449 (11)
β (°)	90.51 (4)
V (Å^3)	803.5 (8)
Z	4
D_x (Mg m^{-3})	1.688
Radiation type	Cu $K\alpha$
Wavelength (Å)	1.54178
No. of reflections for cell parameters	24
θ range (°)	22.5–27.5
μ (mm^{-1})	1.328
Temperature (K)	120 (1)
Crystal form	Thin plate, irregular
Crystal size (mm)	0.30 × 0.30 × 0.01
Crystal color	Colorless

Data collection

Diffractometer	Siemens P4RA
Data collection method	ω scans (3°)
Scan speed (° min^{-1})	11
Absorption correction	XABS2 (Parkin et al., 1995)
T_{min}	0.67
T_{max}	0.98
No. of measured reflections	1147
No. of independent reflections	954
No. of observed reflections	808
Criterion for observed reflections	$I > 2\sigma(I)$
R_{int}	0.0736
θ_{max} (°)	53.48
Mean $I/\sigma(I)$	16.8
Range of h, k, l	$-7 \rightarrow h \rightarrow 7$
	$0 \rightarrow k \rightarrow 6$
	$0 \rightarrow l \rightarrow 18$
No. of standard reflections	2
Frequency of standard reflections	Every 198 reflections
Intensity decay (%)	<1% fluctuation

Refinement

Refinement on	F^2
R_1[on F for $I > 2\sigma(I)$]	0.0406
$wR(F^2)$	0.1094
S	1.078
No. of reflections used in refinement	954
No. of parameters used	141
H-atom treatment	Riding on UA, restrained on water
Weighting scheme	$w = 1/[\sigma^2(F_o^2) + (0.050P)^2 + 0.514P]$, where $P = (F_o^2 + 2F_c^2)/3$
$(\Delta/\sigma)_{max}$	0.000
$\Delta\rho_{max}$ (e Å^{-3})	0.171
$\Delta\rho_{min}$ (e Å^{-3})	−0.152
Extinction method	None
Source of atomic scattering factors	International Tables for Crystallography (Vol. C)

Computer programs

Data collection	P3/PC (Siemens, 1989a)
Cell refinement	XDISK (Siemens, 1989b)

Table 1 (cont.)

Data reduction	XDISK, XPREP (Siemens, 1989b)
Structure solution	SHELXS86 (Sheldrick, 1990)
Structure refinement	SHELXL93 (Sheldrick, 1993)
Preparation of material for publication	SHELXTL (Sheldrick, 1984)

refinement was poor ($R_1 \simeq 21\%$) and all further work used dataset 2. Refinement with version 4.21 of SHELXTL (Sheldrick, 1984) proceeded smoothly to an anisotropic model (138 parameters), but the R index [based on 'observed data', i.e. $F > 4\sigma(F)$] would not drop below $\sim12\%$. There were also unacceptably large peaks (~1.1 e Å^{-3}) remaining in difference-Fourier maps and anisotropic displacement parameters (ADP's) were visibly distorted.

3.1. Twinning

Pseudo-orthorhombic twinning relating (h,k,l) to $(\bar{h},\bar{k},l)$ was investigated by refinement against F^2 using all data with SHELXL93 (Sheldrick, 1993). The addition of a single variable to refine twin fractions (Pratt et al., 1971; Jameson, 1982) resulted in an improved fit ($R_1 = 0.0699$, 'observed data', 139 parameters) and slightly smaller, but still distorted ADP's. The remaining difference map peaks were smaller (~0.80 e Å^{-3}), but not enough to inspire full confidence.

3.2. Disorder

The residual electron density peaks and distorted ADP's were consistent with a twofold rotation of UA, similar to that in AMG. Refinement of a twinned and disordered model with isotropic U's gave a dramatically superior fit with far fewer parameters. This disorder model was created by transformation of the major component coordinates (x, y, z) to $(\frac{1}{2} - x, 1 - y, z)$, so only one more least-squares parameter was needed for their occupancies. Two anisotropic models were also investigated. In the first, refined ADP's of the major component were applied to the minor after taking the transformation into account. In the second, minor component atoms were assigned the isotropic U_{eq}'s of their major component equivalents. The second model was dismissed due to marginally worse R_1 and min/max $\Delta\rho$, despite the equal number of parameters. R_1 indices were 0.0453 (81 parameters) for the isotropic UA model and 0.0406 (141 parameters) for the best anisotropic model. The largest residual electron density map features were 0.25 and -0.18 (isotropic UA), and 0.17 and -0.15 e Å^{-3} (anisotropic). The two water O atoms retained their ADP's thoughout. As a further check, the disordered isotropic UA model was refined without twinning, but this was less satisfactory ($R_1 = 0.0765$, $\Delta\rho_{max} = 0.26$ e Å^{-3}, 80 parameters). Since the disorder

model required only one more least-squares parameter, we are confident that the large reduction in R_1 for the twinned and disordered model is not a consequence of the data:parameter ratio. H-atom positions of the two disorder components are surprisingly close (Fig. 1) and were found in difference maps. They were refined using a riding model with U values tied to those of their connecting atoms. Water H atoms were located in difference maps using Xfit from the XtalView package (McRee, 1992) and refined with distance and angle–distance restraints, and U tied to their O atoms.

4. Results and discussion

Pseudo-orthorhombic twinning is not uncommon in monoclinic crystals with β very close to $90°$ (Dunitz, 1964). When the fraction of twin components differs by more than ~20–30%, diffraction from the smaller component manifests itself as apparently random noise on intensities of the larger component (Jameson, 1996). Consequently, structure solution is often possible, but refinement is rarely satisfactory (Pratt et al., 1971).

Treatment of the AMG model in Pnab forces a 50:50 average of disorder components, making resolution of the separate components tricky. In the AMG model it was noted that the superposition of atoms was not perfect. The resulting skewed electron densities in
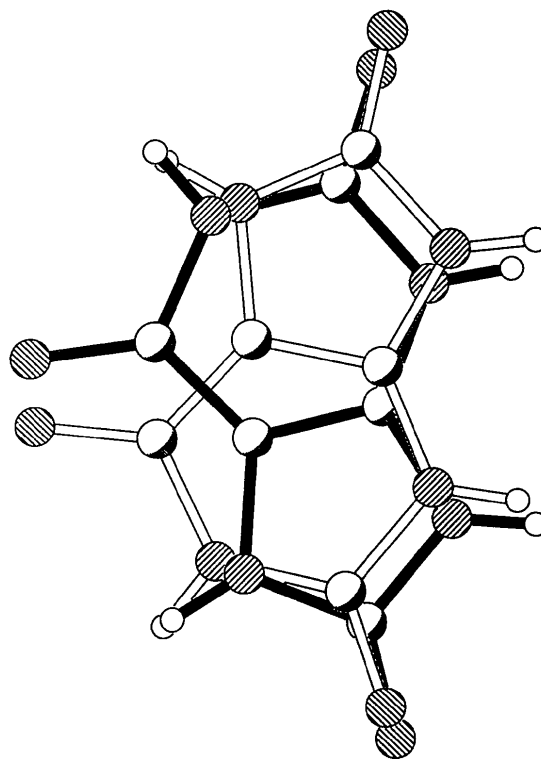

Fig. 1. The nature of disorder in uric acid dihydrate at 120 K.

AMG were accounted for with ADP's, giving a severely distorted structure which nevertheless had very reasonable agreement statistics. In our model the refined disorder fractions of 0.83 and 0.17 agree well with the size of the residual difference density peaks before the disorder model was incorporated. We were thus able to refine the main component freely (Fig. 2a) and tie the smaller component (Fig. 2b). Since the β angle is not quite 90°, mapping (x, y, z) of the major component to $(\frac{1}{2} - x, 1 - y, z)$ of the minor introduces some very slight distortion, which is insignificant at this level of accuracy and precision (Tables 2 and 3).

As with AUA (Ringertz, 1966) and the AMG model, the molecule of UA is in the tri-keto form with bond lengths slightly longer for carbonyl bonds in the six-membered ring (Table 3). This is slightly at odds with the structure of AUA, but the differences are within the uncertainty limit imposed by spherical-atom scattering factors (Coppens et al., 1969). The overall geometry of the uric acid molecule agrees with both AUA and the
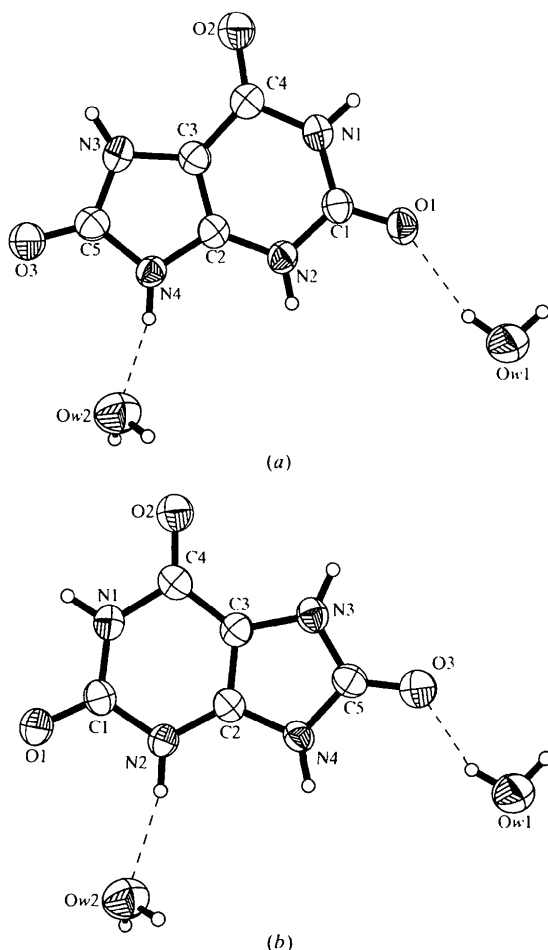
(a)

(b)

Fig. 2. The refined (a) major and (b) minor disorder components (0.83 and 0.17) in UAD at 120 K. Thermal ellipsoids are at the 50% probability level. Dashed lines denote hydrogen bonds to water molecules.

Table 2. *Fractional atomic coordinates and equivalent isotropic displacement parameters* $(\mathring{A}^2)$

$U_{eq} = (1/3)\Sigma_i\Sigma_j U^{ij} a^i a^j \mathbf{a}_i.\mathbf{a}_j$.

Major UA component only. The minor component was formed via the non-crystallographic transformation (x, y, z) to $(\frac{1}{2} - x, 1 - y, z)$.

	x	y	z	U_{eq}
C1	0.1062 (6)	0.2154 (7)	−0.4243 (3)	0.0363 (11)
C2	0.2566 (6)	0.5322 (6)	−0.4014 (2)	0.0329 (10)
C3	0.2840 (5)	0.5691 (6)	−0.4772 (2)	0.0361 (11)
C4	0.2242 (5)	0.4272 (6)	−0.5329 (3)	0.0361 (11)
C5	0.4035 (6)	0.8378 (7)	−0.4121 (3)	0.0385 (12)
N1	0.1394 (5)	0.2520 (5)	−0.4997 (2)	0.0371 (10)
H1†	0.1039 (5)	0.1553 (5)	−0.5309 (2)	0.045
N2	0.1717 (5)	0.3611 (5)	−0.3730 (2)	0.0348 (9)
H2†	0.1590 (5)	0.3439 (5)	−0.3244 (2)	0.042
N3	0.3742 (5)	0.7627 (5)	−0.4831 (2)	0.0377 (9)
H3†	0.4055 (5)	0.8234 (5)	−0.5250 (2)	0.045
N4	0.3316 (4)	0.6965 (5)	−0.3612 (2)	0.0333 (9)
H4†	0.3334 (4)	0.7090 (5)	−0.3121 (2)	0.040
O1	0.0226 (4)	0.0561 (5)	−0.4020 (2)	0.0414 (8)
O2	0.2400 (4)	0.4442 (4)	−0.60374 (15)	0.0417 (8)
O3	0.4815 (4)	1.0053 (5)	−0.3958 (2)	0.0427 (8)
H1	0.3960 (5)	0.8443 (5)	−0.5308 (2)	0.044
H2	0.3414 (5)	0.6568 (5)	−0.3244 (2)	0.042
H3	0.0942 (5)	0.1761 (5)	−0.5251 (2)	0.045
H4	0.1669 (4)	0.2917 (5)	−0.3121 (2)	0.040
Ow1	−0.0899 (4)	−0.2046 (5)	−0.2775 (2)	0.0620 (8)
H1w1‡	−0.050 (6)	−0.107 (5)	−0.307 (2)	0.093
H2w1‡	−0.124 (7)	−0.298 (6)	−0.310 (2)	0.093
Ow2	0.4040 (4)	0.7714 (5)	−0.2155 (2)	0.0653 (9)
H1w2‡	0.340 (6)	0.839 (6)	−0.184 (2)	0.098
H2w2‡	0.425 (7)	0.652 (4)	−0.195 (3)	0.098

† U is constrained to $1.2U_{eq}$ of the connecting N atom. ‡ U is constrained to $1.5U_{eq}$ of the connecting O atom.

AMG model, despite the distortions in the latter. Given the appropriate cell transformation and the different treatment of disorder, the description of hydrogen-bonded ribbons in AMG is very similar to that found here. These ribbons form planes separated by layers of water (Figs. 3a and b), in complete agreement with AMG. Water molecules are hydrogen-bonded to UA via both N2 and N4, and via all three UA O atoms. O1 and O3 form a single hydrogen bond (to either water depending on the disorder component), whereas O2 coordinates to both. As a consequence of UA disorder, it is very likely that some disorder of the waters remains unresolved. Evidence of this lies in both the water oxygen displacement parameters, which are somewhat higher than those of UA (Table 2) and also in the rather distorted UA–water hydrogen bonds for the minor component (Table 4).

The known epitaxy of AUA and UAD is easily explained by the similarity of a and b axes of AUA (after transformation) with the b and a axes of UAD given here, and agrees well with AMG. It is noteworthy, however, that the monoclinic β angle in UAD at 120 K is identical to that of AUA after transformation.

It is interesting to speculate on the processes occurring on a molecular level during growth of UAD crys-

Table 3. *Interatomic distances (Å) and angles (°) in UAD at 120 K*

UA H atoms were placed at calculated positions and for brevity are not included here.

	Major	Minor
C1—O1	1.244 (5)	1.241 (5)
C1—N1	1.358 (6)	1.354 (6)
C1—N2	1.371 (6)	1.377 (6)
C2—N2	1.347 (5)	1.343 (5)
C2—C3	1.359 (6)	1.356 (6)
C2—N4	1.369 (5)	1.374 (5)
C3—C4	1.393 (6)	1.397 (5)
C3—N3	1.398 (5)	1.398 (6)
C4—O2	1.248 (5)	1.246 (5)
C4—N1	1.400 (5)	1.396 (5)
C5—O3	1.238 (5)	1.240 (5)
C5—N3	1.343 (6)	1.347 (6)
C5—N4	1.369 (6)	1.363 (6)

	Water 1	Water 2
Ow—H1w	0.86 (2)	0.85 (2)
Ow—H2w	0.84 (2)	0.85 (2)

O1—C1—N1	122.2 (4)	121.8 (4)
O1—C1—N2	120.8 (4)	121.0 (4)
N1—C1—N2	116.9 (4)	117.2 (4)
N2—C2—C3	124.7 (4)	124.3 (4)
N2—C2—N4	127.5 (3)	127.6 (3)
C3—C2—N4	107.8 (4)	108.1 (4)
C2—C3—C4	121.3 (4)	121.5 (4)
C2—C3—N3	107.2 (4)	106.8 (4)
C4—C3—N3	131.5 (4)	131.7 (4)
O2—C4—C3	127.2 (4)	127.4 (4)
O2—C4—N1	121.6 (4)	121.2 (4)
C3—C4—N1	111.2 (4)	111.4 (4)
O3—C5—N3	125.8 (4)	126.2 (4)
O3—C5—N4	126.3 (4)	126.1 (4)
N3—C5—N4	107.9 (4)	107.7 (4)
C1—N1—C4	128.2 (4)	127.9 (4)
C2—N2—C1	117.5 (4)	117.7 (4)
C5—N3—C3	108.4 (4)	108.8 (4)
C5—N4—C2	108.7 (4)	108.6 (4)

	Water 1	Water 2
H1w—Ow—H2w	102.2 (4)	106.3 (4)

tals. Within a given twin component, there is some probability that a molecule will incorporate in a flipped orientation, leading to disorder. If subsequent molecules also incorporate in the flipped orientation, then the net effect is growth of the twin. Furthermore, it is reasonable to assume that the ability of a UAD crystal to accommodate disorder is dependent upon the nature of the growth medium (*i.e.* pH, temperature, concentration, impurities *etc.*). Strain built up by disordering of UA is offset to some extent by relaxation of the water molecules. The variable systematic absences observed by Ringertz (1965) imply that twinning and disorder fractions can vary from crystal to crystal. Slight differences in the environments of the disorder components will likely affect the rate of water loss in crystals with different disorder fractions and may be related to variations in stability for crystals from different sources.

Table 4. *Hydrogen-bonding distances in UAD at 120 K*

A and B refer to the major and minor components, respectively.

O1—Ow1	2.858 (5)
N2A^i—Ow1	2.729 (5)
O2A^{ii}—Ow1	2.785 (5)
N4A—Ow2	2.634 (5)
O2A^{iii}—Ow2	2.920 (6)
O3A^{iv}—Ow2	2.702 (5)
N1A—O1A^i	2.851 (5)
N1A—O3B^i	2.651 (5)
N3A—O3A^v	2.789 (5)
N3A—O1B^v	2.949 (5)
O3B—Ow1	2.553 (4)†
N4B^i—Ow1	2.491 (5)†
O2B^{ii}—Ow1	3.280 (5)†
N2B—Ow2	2.921 (5)†
O2B^{iii}—Ow2	2.477 (6)†
O1B^{iv}—Ow2	3.042 (5)†
N1B—O1B^v	2.863 (5)
N1B—O3A^v	2.671 (5)
N3B—O3B^{ii}	2.775 (5)
N3B—O1A^{ii}	2.936 (5)

Symmetry codes: (i) $-x, 1 + y, -1 - z$; (ii) $-x, -y, -1 - z$; (iii) $x, \frac{3}{2} - y, -\frac{1}{2} + z$; (iv) $1 - x, -\frac{1}{2} - y, -\frac{1}{2} - z$; (v) $1 - x, -\frac{1}{2} + x, -1 - z$. † These values are likely distorted owing to the lack of a suitable disorder model for the water molecules.
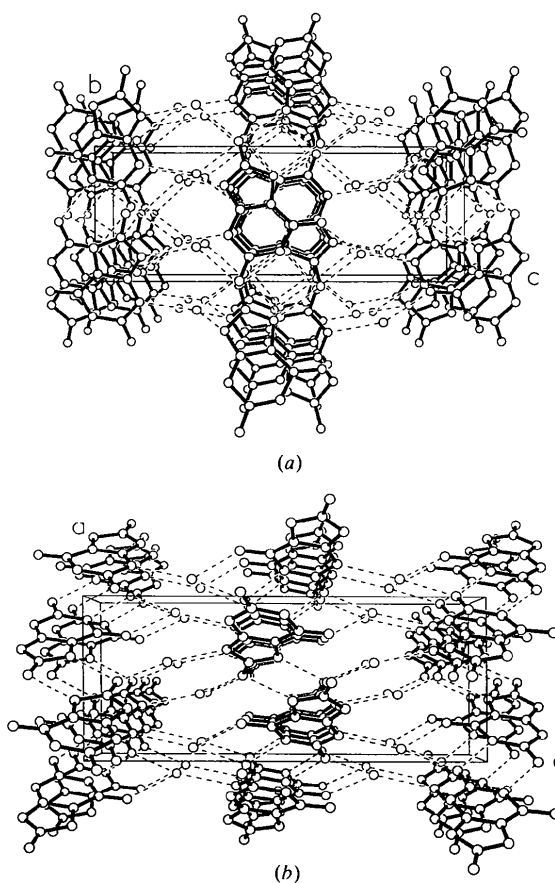

(a)

(b)

Fig. 3. The packing arrangement in UAD at 120 K. (a) View down the crystallographic a axis; (b) view down the b axis.

References

Artioli, G., Masciocchi, N. & Galli, E. (1997). *Acta Cryst.* B53, 498–503.

Coppens, P., Sabine, T. M., Delaplane, R. G. & Ibers, J. A. (1969). *Acta Cryst.* B25, 2451–2458.

Dunitz, J. (1964). *Acta Cryst.* 17, 1299–1304.

Hope, H. (1987). In *Experimental Organometallic Chemistry: A Practicum in Synthesis and Characterization*, edited by A. L. Wayda & M. Y. Darensbourg. Am. Chem. Soc. Symp. Ser. No. 357, ch. 10, pp. 257–262.

Jameson, G. B. (1982). *Acta Cryst.* A38, 817–820.

Jameson, G. B. (1996). Abstract MS02-01-17, p. C43. International Union of Crystallography XVII Congress and General Assembly, Seattle, WA, USA.

Lonsdale, K. & Mason, P. (1966). *Science*, 152, 1511–1512.

McRee, D. E. (1992). *J. Mol. Graphics*, 10, 44–46.

Parkin, S., Moezzi, B. & Hope, H. (1995). *J. Appl. Cryst.* 28, 53–58.

Pratt, C. S., Coyle, B. A. & Ibers, J. A. (1971). *J. Chem. Soc. A*, pp. 2146–2151.

Rinaudo, C. & Boistelle, R. (1980). *J. Cryst. Growth*, 49, 569–579.

Ringertz, H. (1965). *Acta Cryst.* 19, 286–287.

Ringertz, H. (1966). *Acta Cryst.* 20, 397–403.

Sheldrick, G. M. (1984). *SHELXTL User's Manual*. Revision 4.1. Nicolet XRD Corporation, Madison, Wisconsin, USA.

Sheldrick, G. M. (1990). *Acta Cryst.* A46, 467–473.

Sheldrick, G.M. (1993). *SHELXL93. Program for the Refinement of Crystal Structures*. University of Göttingen, Germany.

Shirley, R. (1966). *Science*, 152, 1512–1513.

Siemens (1989a). *P3/PC Diffractometer Program*. Version 3.13. Siemens Anayltical X-ray Instruments Inc., Madison, Wisconsin, USA.

Siemens (1989b). *XDISK. Data Reduction Program*. Version 3.11. Siemens Anayltical X-ray Instruments Inc., Madison, Wisconsin, USA.

Sutor, D. J. & Scheidt, S. (1968). *Br. J. Urol.* 40, 22–28.